# Magnetic interactions in an ensemble of cubic nanoparticles: A Monte Carlo study

Magdalena Woińska,[1] Jacek Szczytko,[1,*] Andrzej Majhofer,[1] Jacek Gosk,[1,2] Konrad Dziatkowski,[1] and Andrzej Twardowski[1]

[1]*Institute of Experimental Physics, Faculty of Physics, University of Warsaw, Hoza 69, 00-681 Warsaw, Poland*

[2]*Faculty of Physics, Warsaw University of Technology, Koszykowa 75, 00-662 Warsaw, Poland*

(Received 12 June 2013; revised manuscript received 13 September 2013; published 24 October 2013)

The ensemble of spatially disordered and randomly oriented spherical monodispersed single-domain magnetic nanoparticles with cubic anisotropy was studied by the Monte Carlo method. In the presence of dipole-dipole interactions, the effect of both particle volume and interparticle separation was investigated with respect to the characteristic parameters of hysteresis loops and zero field cooled and field cooled magnetization curves. The coercive field and remanent magnetic moment were shown to depend strongly on the dimensionless parameter $\beta = k_B T/(K_1 V)$ ($T$ temperature, $V$ particle volume, $K_1$ cubic anisotropy constant). It was revealed that strong dipole-dipole interactions suppress both the coercive field and the remanent magnetic moment of densely packed nanoparticles. Yet, the effect quickly diminishes with the increasing interparticle distances and becomes rather insignificant for separations exceeding three particle diameters. The blocking temperature was found to be weakly affected by dipolar interactions, but mainly governed via $\beta$, i.e., by the nanoparticle volume and the strength of crystalline anisotropy. The role of dipole-dipole interactions on magnetic properties of nanoparticles was further elucidated by a comparison of the simulation results for a single cluster with an infinite periodic arrangement of such clusters.

DOI: 10.1103/PhysRevB.88.144421 PACS number(s): 75.75.−c, 75.50.Tt

## I. INTRODUCTION

Ferromagnetic nanoparticles and their assemblies belong to systems intensively investigated for many years now. It is mainly due to the expectations that research in this field will result in new technologies ranging from new magnetic materials to new methods in cancer diagnostics and treatment. In particular, nanocomposites with ferromagnetic nanoclusters embedded in a semiconductor matrix are promising candidates for information storage and spin electronics applications. Such ferromagnetic nanocomposites can be produced by controlling the aggregation of magnetic cations in semiconductors, e.g., to mention ferromagnetic MnAs dots embeded in GaAs, obtained by thermal annealing of $Ga_{1-x}Mn_xAs$ epilayers,[1–3] MnN dots in the GaN lattice,[4] or FeN dots in MOVPE-grown (Ga,Fe)N.[5,6] A correct understanding of magnetic properties of rocks containing fine ferromagnetic inclusions is also of great importance in paleomagnetic studies.[7]

However, despite constant progress in both experimental and computational techniques, assemblies of ferromagnetic nanoparticles embedded in a nonmagnetic host are not fully understood yet. An interplay of many different phenomena related to the size, shape, and crystal structure of particles[7–16] results in crystallographic, shape, and surface anisotropy of each particle's magnetic properties. Additionally, due to weak but long-range dipole-dipole interactions between atomic magnetic moments, only the smallest particles occur to be magnetic single domains (e.g., for fcc-Co particles[8] with diameters below, roughly, 20 nm). Furthermore, dipole-dipole interactions between magnetic moments of particles contribute also to the bulk magnetic properties of any macroscopic assembly of ferromagnetic nanoparticles. As a rule, theoretical models of composite materials concentrate on effects most important in the investigated context, and in order to simulate properties of systems of single-domain ferromagnetic particles Monte Carlo simulation techniques are most often used.[17–21] In this way, e.g., systems of noninteracting (no dipole-dipole interactions present) particles with cubic magnetic anisotropy[17,18] and systems of interacting particles but with simple uniaxial anisotropy[19–25] had been investigated.

The aim of this work is to investigate in a systematic way the role of the size of particles and their concentration for magnetic properties of a monodispersed assembly of single-domain particles with full cubic crystallographic anisotropy and interparticle dipole-dipole interactions taken into account. Within the same Monte Carlo scheme, experiments on zero field cooled (ZFC) and field cooled (FC) samples are simulated to estimate blocking temperatures $T_b$; then, with temperature set constant, hysteresis curves are simulated to find saturation and remanent magnetic moments $M_s$ and $M_r$, respectively, as functions of the size and concentration of particles. To better understand the role of interparticle dipole-dipole interactions, results obtained for a single cluster of particles are compared to those for an infinite, periodic system of such clusters. In the last case, Ewald summation techniques are used to properly account for the infinite range of dipole-dipole interactions.[19–21] In this way, we model an infinite heterogeneous medium that consists of randomly distributed ferromagnetic particles embedded in a nonmagnetic host. Furthermore, for each considered configuration of particles, all the calculations are repeated with the particle-particle distances multiplied by the same factor: we start with configurations in which closest particles touch each other (we assign the scaling factor s.f. = 1 to this case) then use factors 2 and 8 (s.f. = 2 and 8, respectively) to rescale the distances. In this way, we are able to compare properties of systems that differ solely in concentration of ferromagnetic particles. All presented results are averages over 20 independently obtained configurations.

To demonstrate the results of our model and to be as close to experimental results as possible, the values of anisotropy parameters as for the bulk fcc-Co are chosen. We assume all particles to form homogeneously magnetized single domains. Although our model is still too simple to directly compare its quantitative outcome with experimental data, the main

 

trends observed in experiments are correctly reproduced. Our results indicate that by changing the size and concentration of ferromagnetic particles, it should be possible to change the system from hard to soft magnet.

The paper is organized as follows. In Sec. II A, the physical content of the considered model is presented and the values of anisotropy constants are discussed. In Sec. II B, the details of the Monte Carlo procedure applied are described, while Sec. II C presents the Ewald summation techniques used. Section III contains results of the calculations. First, in Sec. III A, we present simulations for a single nanoparticle. These, on the one hand, provide a good reference for subsequent discussions of results for systems of such noninteracting particles and, on the other hand, since in this case analytical results are known,[26] serve as additional tests of our numerical procedures. Section III B contains results of simulations for single clusters and infinite, periodic systems of such clusters. Section IV summarizes the conclusions.

## II. COMPUTATIONAL DETAILS

### A. Model

Superparamagnetic cobalt nanoparticles are a complex system in which many interactions of various types can be observed. For this reason, the Monte Carlo (MC) technique is the method of choice as an efficient tool for simulations of systems with multiple degrees of freedom, for which analytical calculations could not be performed. In order to reduce the level of complexity, some assumptions concerning the investigated objects must be made. First, cobalt nanoparticles are assumed of spherical shape with a well-defined uniform diameter and to be homogeneously magnetized. Only single-domain nanoparticles with coherently rotating magnetic moments are considered. Therefore, the total magnetic moment of each nanoparticle can be treated as a point dipole located at the center of the particle. The magnitude of such a dipole is assumed to be equal to the magnetic moment of a bulk, uniformly magnetized piece of fcc-Co with a volume equal to that of the considered nanoparticle. Moments of nanoparticles are allowed to rotate according to the forces acting in the medium, whereas the particles themselves stay motionless.

The Hamiltonian of the described system consists then of three terms:

$$H = H_B + H_{\text{anis}} + H_{\text{dip}}. \tag{1}$$

The first term $H_B$ describes interactions of the moments of particles with external magnetic field and is given by

$$H_B = -\sum_{i=1}^{N} \vec{m}_i \vec{B}, \tag{2}$$

where the sum runs over all $N$ nanoparticles with magnetic moments $\vec{m}_i$ acted upon by external magnetic field $\vec{B}$. Model nanoparticles are considered to have crystallographic structure of bulk fcc-Co. Thus, the second term in the Hamiltonian, which denotes energy of interactions of magnetic moments with crystalline lattice, is given by the expression relevant for the cubic anisotropy:

$$H_{\text{anis}} = V \sum_{i=1}^{N} \left[ K_1 \left( \alpha_{1i}^2 \alpha_{2i}^2 + \alpha_{1i}^2 \alpha_{3i}^2 + \alpha_{2i}^2 \alpha_{3i}^2 \right) + K_2 \left( \alpha_{1i}^2 \alpha_{2i}^2 \alpha_{3i}^2 \right) \right]. \tag{3}$$

In the above formula, $\alpha_{1i}$, $\alpha_{2i}$, and $\alpha_{3i}$ denote the direction cosines of the vector of magnetic moment in the reference frame constituted by three equivalent perpendicular crystallographic axes [100], [010], and [001]. $K_1$ and $K_2$ are cubic anisotropy constants of the first and the second order, respectively, and $V$ is the volume of a single nanoparticle. It is known that $K_1$ and $K_2$ strongly depend on temperature, however, very little suitable data can be found in the literature on this topic. $K_1$ and $K_2$ values at $T = 0$ K extrapolated from experimental results are both negative and amount to $K_1 = -9.0 \times 10^5$ erg/cm$^3$ and $K_2 = -2.0 \times 10^5$ erg/cm$^3$.[27] At the same time, some sources cite only the absolute value of the cubic anisotropy constant of the first order being equal to either $K_1 = 2.6 \times 10^6$ erg/cm$^3$ (Refs. 9 and 28) or $K_1 = 2.7 \times 10^6$ erg/cm$^3$ (Refs. 9 and 17) (giving no information about the temperature to which these values refer). Herein, we accept the negative sign of both constants and use higher value $K_1 = -2.7 \times 10^6$ erg/cm$^3$ in order to strengthen the effects of cubic symmetry. To simplify our model, we neglect effects due to the surface anisotropy of magnetization. In the case of nanoparticles with very small diameters, magnetic moments of atoms located near the surface make a considerable part of the magnetic moment of the whole particle and may be canted due to the interactions on the surface that are different than in the bulk of the considered material. For fcc-Co nanoparticles, surface contribution to the anisotropy energy increases significantly[9] when the diameter decreases below 5 nm and may raise the value of the anisotropy constant 2–3 times.[27,29] As stated above, these effects are not included in our model. What regards $K_2$, the above-quoted extrapolation to 0 K is used in the calculations for any $T$. As a consequence of these assumptions, each particle has four easy axes of magnetization coinciding with the family of equivalent ⟨111⟩ crystallographic directions of fcc-Co and three difficult axes along ⟨100⟩-type directions.

The last term in Eq. (1) describes dipolar interactions between magnetic moments of individual nanoparticles. If $\vec{m}_i$ and $\vec{m}_j$ are magnetic moments, whose positions are designated by vectors $\vec{r}_i$ and $\vec{r}_j$, then $H_{\text{dip}}$ is a sum of dipolar interactions of moments present in the system:

$$H_{\text{dip}} = \frac{\mu_0}{4\pi} \sum_{i<j}^{N} \frac{\vec{m}_i \vec{m}_j r_{ij}^2 - 3(\vec{m}_i \vec{r}_i)(\vec{m}_j \vec{r}_i)}{r_{ij}^5}, \tag{4}$$

where $r_{ij}$ is the distance between the $i$th and $j$th particles and $\mu_0$ is the magnetic permeability of the free space. Computation of the energy of dipolar interactions is substantially more time consuming than computations of energy for the other two types of interactions included in the Hamiltonian. For this reason, a commonly applied approach is to take into account only dipole-dipole interactions within a certain shell of nearest neighbors or disregard them completely, which allows us to perform calculations for larger systems. In the simulations presented in this work, the infinite range of dipole-dipole

interactions is fully taken into account at the expense of restricting the size of the investigated model system to only 27 nanoparticles in the central cell. For this set of particles, periodic boundary conditions are applied to model an infinite medium, while dipole-dipole interactions are accounted for using the procedure of Ewald summation[30] described further in the text.

### B. Monte Carlo method

Monte Carlo simulations were carried out using the standard METROPOLIS algorithm[31,32] applied to a cluster of 27 randomly displaced superparamagnetic fcc-Co nanoparticles. To produce spatial configuration, the following procedure was implemented: first positions of the nanoparticles were chosen randomly subject to the requirement that the surface of each nanoparticle must touch the surface of at least one other particle. Such a cluster of particles is achieved in a procedure of placing the center of a nanoparticle in a randomly selected point of a unit cube surrounding the origin of the coordinate system, and subsequently scaling the nanoparticle's coordinates so that it stops overlapping any of the previously introduced particles. The orientation of crystallographic axes of each of the particles is then chosen randomly. We assign the scaling factor equal to one (s.f. $= 1$) to the obtained configuration. Less concentrated arrangements are obtained via multiplying all the coordinates of nanoparticles by a suitable number larger than one (i.e., changing the scaling factor to s.f. $> 1$). In Fig. 1, we show one of the generated configurations for s.f. $= 1$ [Fig. 1(a)] and s.f. $= 2$ [Fig. 1(b)] with red arrows indicating orientations of crystallographic axes of the type $\langle 100 \rangle$. Once the positions of particles and orientations of their crystallographic axes are chosen, they remain constant within the Monte Carlo run.

One Monte Carlo step (MC step) consists of consecutive, independent, small random deviations of magnetic moments of all particles; after each deviation acceptance conditions are checked according to the prescription of the METROPOLIS algorithm. Random deviation of a magnetic moment is obtained by rotating its vector by $2^\circ$ in a randomly chosen direction. The described procedure allows us to accomplish an arbitrary orientation of a magnetic moment with respect to the global reference frame without favoring any special one. After the values of the external magnetic field and temperature are set, 10 000 MC steps are performed to thermalize the system and then the next 10 000 MC steps are used to calculate the

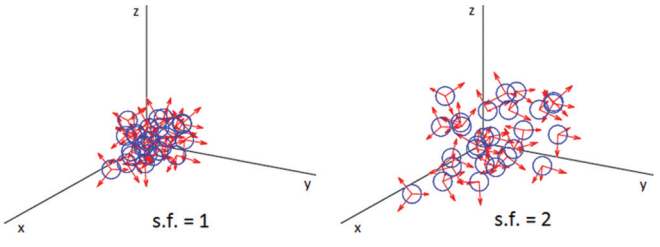


FIG. 1. (Color online) The example of both simulated positions and crystallographic frame orientations for 27 nanoparticles for two different scaling factors. Next, further averaging is taken over 20 independent spatial configurations of nanoparticles.

average value of the magnetic moment of the system. With this choice, we, in a sense, mimic the actual experiments in which constant thermalization and measurement times are kept after each change in the external parameters (i.e., temperature or magnetic field). No special procedure is utilized in order to assure the acceptance of a certain percentage of MC steps since at the temperatures high enough (especially for smaller particles) an arbitrary small deviation of a magnetic moment is accepted with a probability almost equal to 1, and similarly, at higher magnetic fields almost no deviations from the direction of the external field are accepted. According to the results of prior tests published elsewhere,[33] the number of 10 000 MC steps of thermalization and subsequent averaging, although not sufficient to attain equilibrium, is certainly enough to obtain stable values of blocking temperature ($T_b$) and parameters of hysteresis loops such as remanent magnetic moment ($M_r$) and coercive field ($B_c$).

For a given spatial configuration of a system of nanoparticles (Fig. 1) and their magnetic moments, each MC simulation such as calculation of a FC/ZFC curve or hysteresis loop is independently performed 10 times (one individual simulation is called a MC cycle) and then additional averaging over these 10 MC cycles is also performed. Further averaging is taken over 20 independent spatial configurations of nanoparticles. Such a procedure is applied for simulations of all the FC/ZFC curves and hysteresis loops as it allows for smooth computed curves and eliminating effects related with particular configurations in our rather small system of 27 particles.

### C. Ewald summation: An infinite, periodic system

Long-range interactions such as those present in a system of magnetic dipoles are difficult to handle in numerical calculations and substantially increase computational cost due to quadratic growth of the number of interactions with the number of interacting objects. Nevertheless, limiting calculations to a small system including only 27 nanoparticles is a solution carrying the risk of severe underestimation of the role of dipolar interactions and causing effects associated with a limited size of a system to show up. Therefore, an attempt to take into account long-range dipole-dipole interactions is made by means of a standard method known as the Ewald summation.[30] This technique introduces periodicity, which in the case of superparamagnetic nanoparticles is not a characteristic of a system. In this method, a cluster of nanoparticles is put into a supercell being a cube with a minimal edge length sufficient to accommodate a given cluster. The initial supercell, marked by vector $\vec{n} = [0,0,0]$, is surrounded with a lattice of identical cells called supercell images (denoted by vectors $\vec{n} = [n_x,n_y,n_z]$) which create spherical layers. In practice, only a limited number of such layers can be used. Moreover, different spatial configurations of nanoparticles correspond to supercells of slightly distinct sizes, thus averaging over 20 of them additionally weakens possible effects caused by artificially implemented periodicity.

Using Ewald summation, we pursue estimating the energy of interactions of magnetic moments present in a central supercell with one another and with the moments placed in the supercell images. The exact expression for this energy is

the following:

$$E = \frac{1}{2}\frac{\mu_0}{4\pi}\sum_{\vec{n}\in\mathbb{Z}^3}{}' \sum_{i,j=1}^{N}\left(\frac{\vec{m}_i\vec{m}_j}{|\vec{r}_{ij}+\vec{n}L|^3} - \frac{3[\vec{m}_i(\vec{r}_{ij}+\vec{n}L)][\vec{m}_j(\vec{r}_{ij}+\vec{n}L)]}{|\vec{r}_{ij}+\vec{n}L|^5}\right), \quad (5)$$

where the second sum runs over dipole moments in the central supercell, the first sum over vectors $\vec{n}$ with integer coordinates includes all the supercells (the prime indicates that for $\vec{n} = [0,0,0]$ the term $i = j$ is not present in the sum), $\vec{m}_i$ and $\vec{m}_j$ are magnetic moments, and the vector $\vec{r}_{ij}$ is their relative position within the central supercell. $\vec{n}L = [n_x,n_y,n_z]$ symbolizes the position of a certain supercell, while $L$ is the length of its edge. As was already noted, the first sum has to be limited to a certain precisely defined number of vectors, which could cause the emergence of effects associated with forming a surface and appearance of a demagnetizing field. To prevent this behavior, the energy of dipole-dipole interactions must be supplemented with the term $E_{\text{surf}}$ responsible for interactions of the system with external continuum surrounding the finite system of spherical layers and characterized by magnetic permeability of the investigated medium.

The essence of Ewald summation is splitting the energy of dipolar interactions into a short- and a long-range part ($E_r$ and $E_k$, respectively). The first one is a series which can be summed in the direct space and the second one is convergent after transformation to the reciprocal space and in this manner can be summed more effectively. The final expression for the energy of dipole-dipole interactions derived in the formalism of Ewald summation[30,34,35] consists of four components:

$$E = E_r + E_k + E_{\text{self}} + E_{\text{surf}}. \quad (6)$$

The term $E_{\text{self}}$ in this formula is responsible for subtraction of the energy of self-interaction of the dipoles which must be included in $E_k$ before subjecting this component to Fourier transformation to the reciprocal space. We present the resulting expressions for individual components of the Ewald sum in the form derived from the paper by Wang and Holm:[36]

$$E_r = \frac{1}{2}\frac{\mu_0}{4\pi}\sum_{\vec{n}\in\mathbb{Z}^3}{}' \sum_{i,j=1}^{N}\{\vec{m}_i\vec{m}_j B(|\vec{r}_{ij}+\vec{n}L|) - [\vec{m}_i(\vec{r}_{ij}+\vec{n}L)] \times [\vec{m}_j(\vec{r}_{ij}+\vec{n}L)]C(|\vec{r}_{ij}+\vec{n}L|)\}, \quad (7)$$

$$E_k = \frac{\mu_0}{2L^3}\sum_{\vec{l}\in\mathbb{Z}^3,\vec{l}\neq 0}\sum_{i,j=1}^{N}\frac{1}{l^2}e^{-(\frac{\pi l}{\alpha L})^2}(\vec{l}\vec{m}_i)(\vec{l}\vec{m}_j)e^{2\pi i\frac{\vec{l}\vec{r}_{ij}}{L}}, \quad (8)$$

$$E_{\text{self}} = -\frac{2\alpha^3}{3\sqrt{\pi}}\frac{\mu_0}{4\pi}\sum_{i=1}^{N}m_i^2, \quad (9)$$

$$E_{\text{surf}} = \frac{\mu_0}{2(1+2\mu)L^3}\sum_{i,j=1}^{N}\vec{m}_i\vec{m}_j. \quad (10)$$

Functions $B$ and $C$ used in Eq. (7) are defined in the following way:

$$B(r) = \frac{1}{r^3}\left(\text{erfc}(\alpha r) + \frac{2\alpha r}{\sqrt{\pi}}e^{-\alpha^2r^2}\right), \quad (11)$$

$$C(r) = \frac{1}{r^5}\left(3\,\text{erfc}(\alpha r) + \frac{2\alpha r}{\sqrt{\pi}}(3+2\alpha^2r^2)e^{-\alpha^2r^2}\right), \quad (12)$$

where $\text{erfc}(x) := \frac{2}{\sqrt{\pi}}\int_x^\infty e^{-t^2}dt$ is the complementary error function. Vectors $\vec{l}$ introduced in Eq. (8) denote positions of supercells of the reciprocal space. The coefficient $\alpha$ is a parameter which can be adjusted to make Ewald summation optimal for the considered system.[36] In this work, the standard value $\alpha = \frac{5}{L}$ was chosen.[30] Two other parameters responsible for convergence and efficiency of calculations are summation cutoffs in the direct and reciprocal space. In most cases, limiting summation to the central supercell ($\vec{n} = [0,0,0]$) for $E_r$ and summing over 100–200 vectors $\vec{l}$ for $E_k$ is sufficient.[30] In this work, a few values of cutoff coefficients were investigated, however, the quoted minimal values turned out to be the best compromise between accuracy and speed of calculations.

In Eq. (10), $\mu$ denotes relative magnetic permeability of the studied medium. This quantity, though initially unknown, can be estimated iteratively in the course of simulations (in the absence of external magnetic field) as it is related to the standard deviation $s_M$ describing magnetic moment fluctuations by the following formula:

$$\mu = 1 + \frac{\mu_0 s_M^2}{3kTL^3}, \quad \chi_m = \mu - 1, \quad (13)$$

$$s_M^2 = \langle M^2\rangle - \langle M\rangle^2, \quad \vec{M} = \sum_{i=1}^{N_{\text{MC}}}\vec{M}_i \quad (14)$$

in which $k$ is the Boltzmann constant, $T$ is temperature, $\chi_m$ is magnetic susceptibility, $L$ symbolizes the edge length of the supercell, and $\vec{M}_i$ is the total magnetic moment of the system in the $i$th MC step included in averaging ($1 \leqslant i \leqslant N_{\text{MC}}$, for number of $N_{\text{MC}}$ MC steps). According to literature,[30,36] the best preliminary assumption is $\mu = \infty$, eliminating $E_{\text{surf}}$. It turns out that in the case of the studied system of cobalt nanoparticles, one can confine to the first three terms of Eq. (6) since the contribution of $E_{\text{surf}}$ to the total energy is insignificant and can be disregarded.

## III. RESULTS

### A. Single ferromagnetic nanoparticle

Before presenting the results for a many-particle system, a single nanoparticle, the simplest model allowing us to eliminate the influence of interparticle magnetic dipolar interactions, was considered. Such a simplified model is a good starting point for further considerations of changes in properties of a system after including dipole-dipole interactions. It also would be compared to analytical calculations (results based herein on Boltzmann distribution), which serve as a confirmation of correctness of the chosen model.

Simulation of each ZFC curve was always preceded by cooling the system in zero magnetic field from 400 to 2 K. Then, the external magnetic field was turned on and the temperature increased from 2 to 400 K with a 1-K step in order to calculate the ZFC curve. The simulation of the FC curve was performed in the following way: the magnetic field was switched on and remained constant while the temperature was decreased stepwise from 400 to 2 K with a 1-K step. To calculate hysteresis loops, we started from $B = 0$ T. Then, the magnetic field was ramped up to $B = 6$ T, subsequently

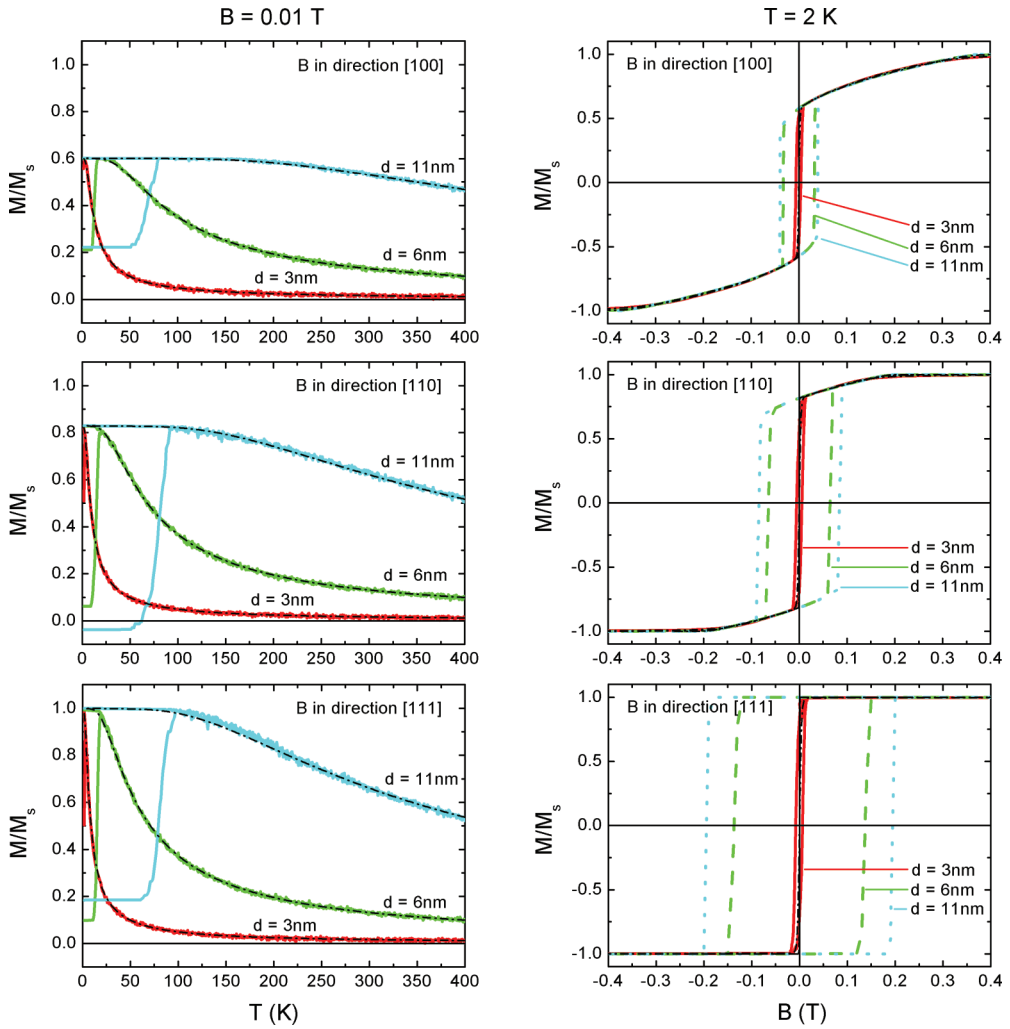


FIG. 2. (Color online) Simulations for a single nanoparticle averaged over 500 000 MC steps. Results shown are for particle diameter $d = 3$, 6, and 11 nm and three different orientations of magnetic field along the crystallographic directions [100], [110], and [111]. Left panel: FC/ZFC curves for $B = 0.01$ T. Right panel: hysteresis loops of a single nanoparticle versus magnetic field $B$ for $T = 2$ K. Black curves represent the corresponding equilibrium values obtained analytically on the basis of Boltzmann distribution.

was decreased stepwise to $B = -6$ T, to be finally increased again to $B = 6$ T. Such a simulation was performed at a fixed temperature and with a step in magnetic field value adjusted to provide more accurate sampling in the region of magnetic moment flipping (step = 0.05 T for $|B| > 0.5$ T, step = 0.01 T for 0.05 T $< |B| <$ 0.5 T, step 0.001 T for $|B| <$ 0.05 T). $T_b$ was read from a FC/ZFC plot as the lowest temperature at which FC and ZFC curves match each other and $M_r$ is read as the magnetic moment of a sample attained in a hysteresis loop, when the external magnetic field is reduced to zero.

Figure 2 presents both results of FC/ZFC simulations (at 0.01 T) and hysteresis curves (at 2 K) calculated for a single nanoparticle in magnetic field. The particles of diameters $d = 3$, 6, and 11 nm are presented. The vector of external magnetic field was aligned in three special crystallographic directions: [100] (maximum of the energy of the anisotropy $E_{\text{anis}}$), [110] (saddle point of $E_{\text{anis}}$), and [111] (minimum of $E_{\text{anis}}$). The number of MC steps was set to $N_{\text{MC}} =$ 500 000 and averaging over 100 MC cycles was performed in order to make the curves smoother. The obtained curves are compared to analytical calculations of magnetic moment at a given temperature and magnetic field obtained from the Boltzmann distribution. The Boltzmann distribution gives information about an equilibrium average value of magnetic moment along the direction of magnetic field, not about local energetic minima and nonequilibrium phenomena; therefore, ZFC curves or hysteresis loops can not be obtained in this way.

It can be observed that the FC curve closely follows the curve representing analytical calculations on the basis of the Boltzmann distribution. Blocking temperature $T_b$ does not change with the direction of magnetic field for particles of diameters 3 and 6 nm. Only for the largest nanoparticles considered (11 nm), $T_b$ grows slightly with the external magnetic field vector changing from the hard to the easy direction of magnetization. It is probable that just in the case of 11-nm nanoparticles, the changes of $E_{\text{anis}}$ with rotation of magnetic moments are large enough (compared to $k_B T$) to cause this slight difference in $T_b$. Another remarkable observation is the upward shift of the maximum of FC curve when magnetic field is rotated from the hard to the easy axis of magnetization.

The ZFC curve simulated for a single particle meets the FC curve at lower $T_b$ than it is observed in the case of simulations for 27 noninteracting nanoparticles (cf. Sec. III B1). This effect is not attributed solely to the increased number of MC steps (in comparison with the further described system of 27 nanoparticles, for which averaging is over 10 000 MC steps and 10 MC cycles), as preceding tests proved that for a single nanoparticle this value is still too low to cause decrease of blocking temperature as large as observed in our simulations. It could rather be explained by the fact that in an assembly of 27 nanoparticles, orientations of crystallographic axes are distributed randomly and $T_b$ corresponds to the temperature at which the most strongly blocked magnetic moment overcomes the anisotropy barrier. However, the presence of other moments (i.e., neighboring magnetic particles), which can be unblocked more easily, pushes the FC curve to higher values (as it can be concluded from Fig. 2) making the conditions of free rotation harder to fulfill for the most strongly blocked moments. As a consequence, blocking temperature in an assembly of particles grows.

In 2 K, the results of simulations of hysteresis loops are in good agreement with analytical calculations on the basis of Boltzmann distribution beyond the range of values of $B$ at which an open loop is observed. Coercive field and remanence grow when the vector of magnetic field moves from the position of the highest $E_{\text{anis}}$ to the lowest. The maximal value of the magnetic moment is achieved at lower field if $\vec{B}$ is closer to the easy axis of magnetization. For particles with $d = 11$ nm (the corresponding $T_b > 100\ \text{K} \gg 2\ \text{K}$), hysteresis curves presented here are in accordance with analytical calculations of Joffe and Heuberger[26] for a system of randomly oriented, noninteracting single-domain particles with cubic anisotropy at $T = 0$ K. It can also be observed that, like for a dilute assembly of 27 nanoparticles with negligible dipolar interactions (cf. Sec. III B2), the reduced magnetic remanence is almost independent of the size of a nanoparticle at 2 K, which is consistent with the fact that in 0 K, magnetic remanence of an assembly of noninteracting nanoparticles has a certain constant value independent of the size.[7,37]

### B. System of interacting ferromagnetic nanoparticles

In the following part of this paper we present FC/ZFC curves simulated in $B = 0.01$ T and hysteresis loops collected for a cluster of 27 identical fcc-Co nanoparticles. Our Monte Carlo calculations were always organized in a way as close to real experiments (cf., e.g., Ref. 38) as possible within the model considered. To better investigate the role of dipole-dipole interactions, we compare results for different configurations for a single cluster with those for an "infinite medium" obtained by applying periodic boundary conditions and Ewald summations. Simulation of ZFC/FC curves and hysteresis loops was always performed in a way already described in Sec. III A for the case of a single ferromagnetic nanoparticle. We consider various diameters of nanoparticles and also various concentrations represented by a series of different values of the scaling factor (s.f.). Several values of temperature and external magnetic field were taken into account. Parameters read from the resulting curves, such as blocking temperature ($T_b$), remanent magnetic moment ($M_r$), and coercive field ($B_c$) are examined for different diameters (3, 6, and 11 nm), scaling factors (s.f. = 1, 1.2, 1.5, 2, 3, 4, 5, 6, 7, 8), and varying external magnetic field $B$ ($T_b$) and temperature $T$ ($M_r$ and $B_c$).

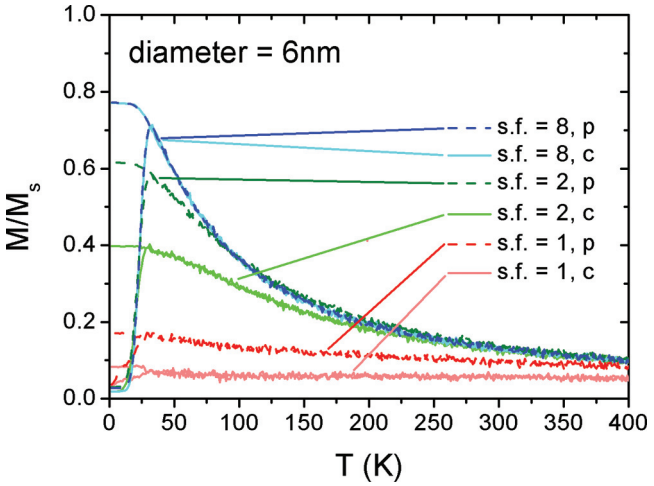


FIG. 3. (Color online) ZFC/FC curves simulated at B = 0.01 T for 6-nm nanoparticles and various scaling factors (s.f. = 1, 2, 8). Single-cluster calculations are marked with "c" (solid lines), while results for the infinite (i.e., periodic) system of such clusters are marked with "p" (dashed lines). 27 nanoparticles, 10 000 MC steps.

#### 1. ZFC/FC experiment

Simulations for three characteristic values of scaling factor are presented. These values of s.f. determine the diminishing contribution of dipolar interactions to the overall energy (s.f. = 1 corresponds to the strongest possible dipolar interactions, s.f. = 2 refers to lower but still non-negligible contribution, and finally for s.f. = 8 interactions of magnetic dipoles can be disregarded). From Fig. 3 it can be noticed that for the most sparsely distributed nanoparticles (s.f. = 8), there is no visible difference between calculations with and without applying periodic boundary conditions and Ewald summation procedures (curves s.f. = 8,p and s.f. = 8,c, respectively). In the case of higher concentrations, we observe a general increase in magnetic moment of FC/ZFC curves that follows adding periodic boundary conditions. The increase is the stronger the more densely the particles are packed: for periodic calculations with s.f. = 1, the magnetic moment attained in 2 K becomes (respectively) twice as high and half as much for nonperiodic calculations. At the same time, increasing concentration causes lowering of the values of magnetic moment of the simulated curves. One possible explanation of this phenomenon is based on the analysis of the influence of short-range dipolar interactions. The energy associated with the short-range part of dipolar interactions changes with an increasing scaling factor but is not effected by using the Ewald sum as a cutoff radius in the direct space used in the calculations $r_c = 0$. In general, a system of Co nanoparticles is characterized by ferromagnetic behavior and additional long-range dipolar interactions added by the Ewald sum strengthen its ferromagnetic properties. However, if we consider a set of 27 nanoparticles, the influence of a limited size of the system on the role of short-range interactions (surface

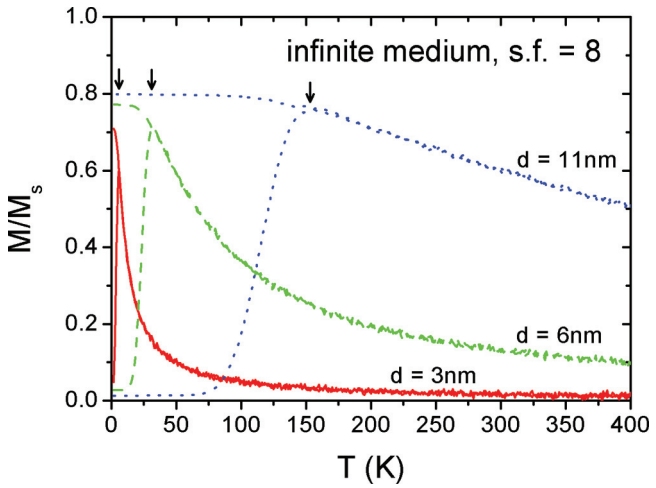


FIG. 4. (Color online) ZFC/FC curves simulated at $B = 0.01$ T for the concentration corresponding to s.f. $= 8$. Vertical arrows indicate values of $T_b$ for nanoparticles with diameters equal to 3, 6, and 11 nm. 27 nanoparticles, 10 000 MC steps.

effects) starts to become important. This effect is more intense for smaller s.f. since in this case short-range interactions are stronger. The other explanation can be the fact that the stronger short-range dipole-dipole interactions block rotation of moments of nanoparticles more effectively. Therefore, in the course of FC/ZFC or hysteresis curve simulation the next minimum to which a magnetic moment jumps after a series of MC steps is more determined by short-range interactions than by external magnetic field and, consequently, the magnetic remanence of a system with stronger short-range interactions is decreased.

The specified trends are well visible in Fig. 3 which depicts FC/ZFC curves for various concentrations calculated with and without using the Ewald summation procedure for 6-nm particles. This figure also shows that the variability of blocking temperature with the scaling factor is rather insignificant, particularly if compared to a huge increase in $T_b$ with the particles' size presented in Fig. 4.

Generally, for the lowest temperatures (i.e., below $T_b$), FC curves are characterized by a high, roughly constant value of magnetic moment and its drop before crossing the blocking temperature. On the other hand, ZFC curves in 2 K start from a low value of magnetic moment along the external magnetic field, however, full thermalization to zero of this component of magnetic moment is hardly ever successful. The divergence from zero magnetic moment observed at low $T$ in the ZFC curve is larger for smaller nanoparticles (as even in $T = 2$ K thermal motions of smaller particles are strong enough to rotate their magnetic moments and induce a small magnetization along the direction of external magnetic field) and lower concentrations (since for higher concentrations the short-range component of dipolar interactions is stronger and causes stronger frustration in the system of magnetic moments, which makes magnetization more susceptible to the influence of external magnetic field in $T = 2$ K). Frustration of magnetic moments makes the part of the ZFC curve for $T < T_b$ less smooth for s.f. $= 1$ than for s.f. $= 2$ or s.f. $= 8$, because of abrupt changes of magnetization resulting from flips of individual moments. At the blocking temperature, the maximum of the ZFC curve is attained and then the FC and ZFC curves match each other, and for $T > T_b$ we observe only one curve which describes freely rotating moments of a superparamagnetic material. After reaching $T_b$, the magnetic moment of the system starts to decrease with growing temperature. The reduction of magnetization is the most rapid for particles with smaller magnetic moments. Blocking temperatures for a given particle size are very similar for different concentrations of nanoparticles and for single clusters and infinite systems.

For a given configuration of particles, in the case when the closest particles touch each other (s.f. $= 1$), all three parts of the Hamiltonian of the system [cf. Eq. (1)] are proportional to the volume $V$ of a single particle. Only the $H_{\text{dip}}$ term decreases with increasing value of s.f. (i.e., particle-particle distance). On the other hand, at temperatures high enough, the considered system of single-domain particles behaves like a paramagnet obeying the simple Curie law. Therefore, the natural graphical method to demonstrate the role of interactions present in a system of nanoparticles is based on the analysis of the product of temperature and magnetic moment (derived from FC/ZFC simulation) versus temperature with both quantities displayed as reduced variables, where reduced blocking temperature is $k_B T_b/2|K_1|V$, $V$ is volume of a nanoparticle, and $K_1$ denotes the first anisotropy constant of fcc-Co. It allows us to determine when the dependence of magnetic moment of a sample starts to follow the simple Curie law, as in a paramagnetic material. Such a graph is presented in Fig. 5. In reduced variables, results of calculations for the same concentration but different sizes (and in the same ranges of nonreduced temperatures) appear as fragments of the same curve. Curves for 11- and 6-nm nanoparticles are superimposed on the curve for the diameter 3 nm and the limits of this superposition (corresponding to $T = 400$ K) are marked by vertical lines. Separate curves are observed only when scaling factors are different. The most characteristic feature of such a curve is its horizontal

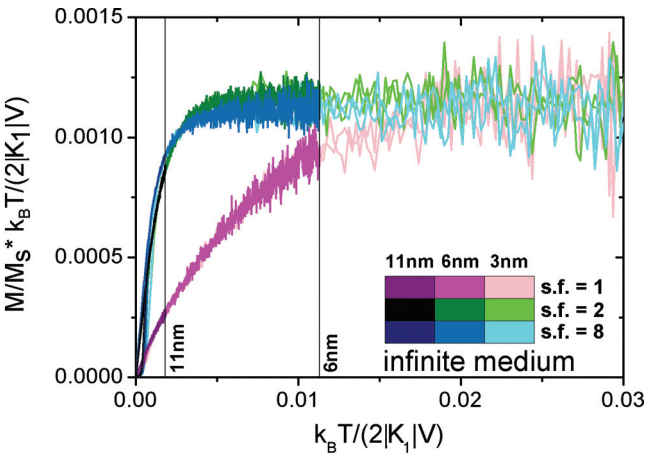


FIG. 5. (Color online) The product of reduced FC/ZFC magnetic moment and reduced temperature $(M/M_s \cdot k_B T/2|K_1|V)$ vs the reduced temperature. Curves for diameters 11 and 6 nm superimposed on curves for 3-nm nanoparticles (limits of superposition corresponding with $T = 400$ K are marked by vertical lines). Tints of magenta: s.f. $= 1$, tints of green: s.f. $= 2$, tints of blue: s.f. $= 8$. 27 nanoparticles, 10 000 MC steps.

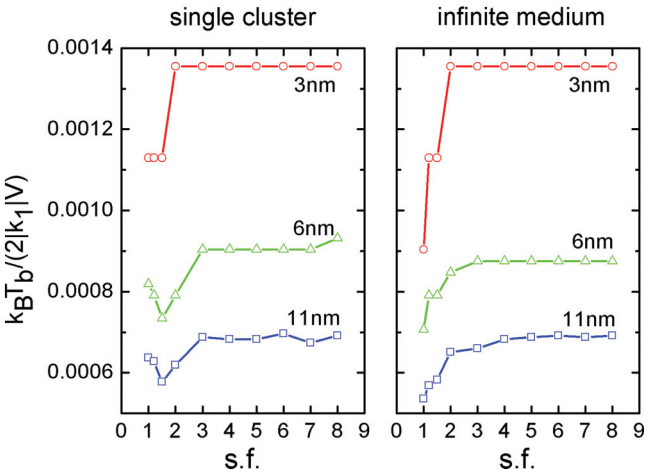


FIG. 6. (Color online) Plot of reduced blocking temperature ($T_b k_B/2|K_1|V$) in $B = 0.01$ T versus scaling factor (s.f.). Sizes of nanoparticles: 3, 6, and 11 nm. 27 nanoparticles, 10 000 MC steps.

course for temperatures high enough to make the role of anisotropy and dipole-dipole interactions nonsignificant and so that magnetic moments could rotate freely as in a paramagnetic material. Such a phenomenon, despite high fluctuations, can be observed for all concentrations considered. As it can be seen, the reduced temperature at which the curve for s.f. = 8 becomes approximately horizontal (if the noise is disregarded) is only slightly lower than that for s.f. = 2. For the most sparsely packed nanoparticles, dipole-dipole interactions are negligible and the temperature at which ZFC/ZFC curves start to resemble a simple Curie law as for a paramagnetic material should be the lowest. For s.f. = 2, this temperature is only slightly higher because dipolar interactions are still quite weak. However, as far as the highest concentration is concerned, flattening of the curve is observed at a significantly higher temperature owing to the stronger role of dipolar interactions. According to the curves in Fig. 5, in the range of temperatures considered in this paper ($T < 400$ K), it is impossible to observe Curie-type character of FC/ZFC curves for 11-nm particles and for 6-nm particles in the case of s.f. = 1.

Figure 6 presents how the reduced blocking temperature depends on the concentration for nanoparticles with diameters of 3, 6, and 11 nm in the external magnetic field $B = 0.01$ T. As a general rule, variation in the $T_b$ with the scaling factor is rather small compared to the changes caused by increasing nanoparticles' size. Therefore, scaling of $T_b$ and presenting its reduced value is necessary to highlight the variability of this parameter for smaller nanoparticles. It also allows us to reveal the different character of the dependence of $T_b$ for s.f. $\leqslant 2$ observed for calculations for a single cluster and for infinite medium (i.e., with and without periodic boundary conditions and Ewald summation procedure). In the case of an infinite system, a slight increase of blocking temperature with the decreasing concentration (i.e., growing s.f.) can be observed for s.f. $\leqslant 4$ for nanoparticles of diameter, respectively, 3, 6, and 11 nm. Simultaneously, in simulations for a single cluster of particles of sizes 6 or 11 nm, there appears a small minimum of $T_b$ for s.f. = 1.5 with $T_b$ decreasing between s.f. = 1 and 1.5 and further increasing between s.f. = 1.5 to 3 and then leveling off. For the smallest nanoparticles, $T_b$ is constant for s.f. $\leqslant 2$, then slightly grows and again remains constant in spite of the decreasing concentration. Although there appear certain tendencies in the dependence of $T_b$ on concentration, it must be stressed that in nonreduced variables these tendencies can be noticed only for the largest particles, while the influence of particles' size on $T_b$ prevails in all the remaining trends. This suggests that when the system of magnetic nanoparticles with cubic anisotropy is dilute enough, the energetic contribution due to magnetocrystalline anisotropy is dominant in the case of blocking of magnetic moments and surpasses the influence of dipolar interactions substantially while, as stated above, the effects of dipole-dipole interactions are visible only for s.f. $\leqslant 3$.

Blocking temperatures decrease rather fast with increasing magnetic field and in most cases for $B = 0.2$ T blocking is not observed. The values of the blocking temperature for a given size of nanoparticles for various concentrations are quite similar, which confirms the dominating influence of magnetocrystalline anisotropy on superparamagnetic behavior of Co nanoparticles. The manifestation of negligible impact of dipolar interactions in systems with low concentrations is the fact that for s.f. = 8, plots of reduced $M_r$ and $B_c$ versus reduced temperature are approximately identical as well as $T_b$ for different magnetic fields.

### 2. *Hystereses*

Typical hysteresis loops calculated at $T = 2$ K are presented in Figs. 7 and 8. For larger scaling factors, the increase of $B_c$ with growing size becomes more significant, while for $M_r$ the tendency is rather opposite, as it can be concluded from Fig. 7. The contribution of more long-range dipole-dipole interactions in an infinite system results in a visible broadening of the loops for s.f. lower or equal to 2 (the effect strengthens with growing concentration) and renders the growth of magnetic moment in a hysteresis loop with the increase of magnetic field faster (Fig. 8). In the case of s.f. = 2, hysteresis loops become much broader compared to s.f. = 1 and the effect of applying periodic boundary conditions for this concentration is rather small.

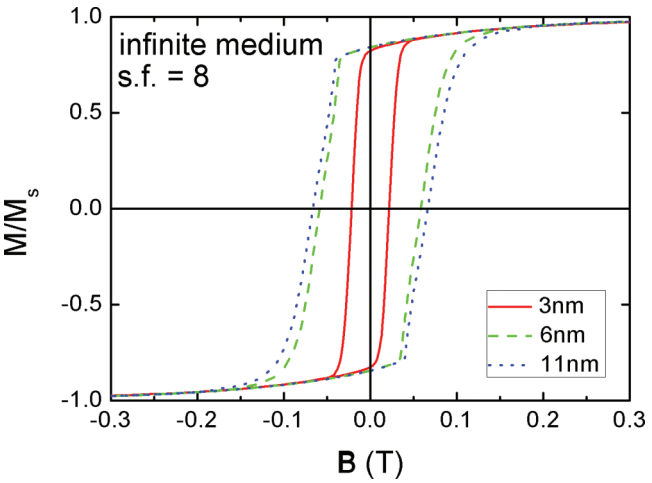


FIG. 7. (Color online) Hysteresis loops simulated in $T = 2$ K, s.f. = 8, infinite system. Sizes of nanoparticles: 3, 6, and 11 nm. 27 nanoparticles, 10 000 MC steps.

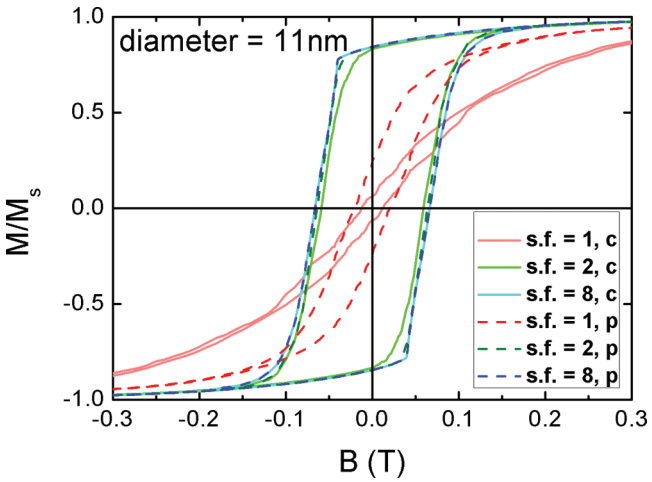


FIG. 8. (Color online) Hysteresis loops simulated in $T = 2$ K for 11-nm nanoparticles and various scaling factors (s.f. = 1,2,8). Single-cluster calculations are marked with "c" (solid lines) and results for an infinite system are marked with "p" (dashed lines). 27 nanoparticles, 10 000 MC steps.

The temperature $T = 2$ K is low enough to observe hysteresis in the case of all the particle diameters and scaling factors discussed in this work. Nevertheless, for nonperiodic calculations and s.f. = 1 in the case of the smallest nanoparticles coercive field and remanence are so low that hysteresis can hardly be noticed (Figs. 9–12). For diameters 6 and 11 nm, $B_c$ and $M_r$ are slightly larger, and their increase depends on concentration. The coercive field $B_c$ is calculated according to the following procedure: in the course of hysteresis loop simulation, when magnetic field is decreased, at some value of magnetic field, the magnetic moment of the system changes sign from positive to negative. We denote by $B_-$ the zero of a straight line going through the following points: the last point for which the magnetic moment is positive and the first point for which the sign of the magnetic moment is negative. Similarly, when the magnetic field is increased, the total moment of the system changes its sign from negative to positive and $B_+$ symbolizes the zero of a line going through

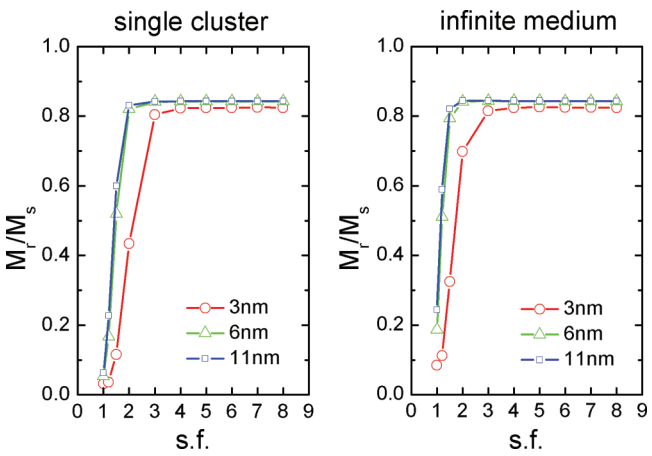


FIG. 9. (Color online) Plot of reduced remanence ($M_r/M_s$) in $T = 2$ K versus scaling factor (s.f.). Sizes of nanoparticles: 3, 6, and 11 nm. 27 nanoparticles, 10 000 MC steps.

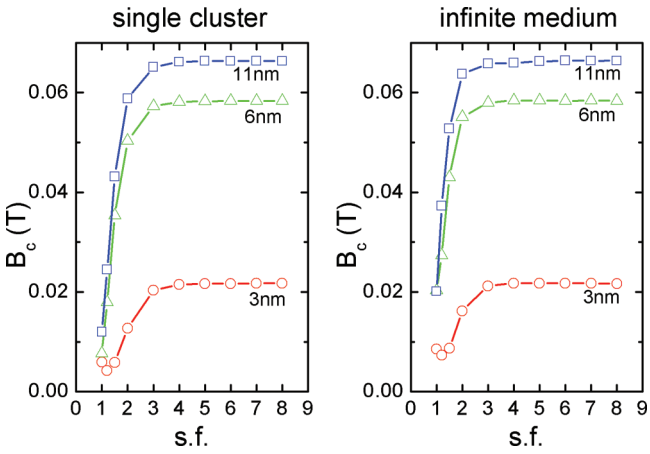


FIG. 10. (Color online) Plot of coercive field ($B_c$) at $T = 2$ K versus scaling factor (s.f.). Sizes of nanoparticles: 3, 6, and 11 nm. 27 nanoparticles, 10 000 MC steps.

the last point with negative and the first point with positive magnetic moment. The coercive field $B_c$ is then calculated as $B_c = (B_+ - B_-)/2$, and it can be slightly negative in the simulations in which the hysteresis loop does not open. Taking into account more long-range interactions makes $M_r$ and $B_c$ for 3-nm nanoparticles and s.f. $\leqslant 2$ larger (Figs. 9 and 10). As far as larger particles are concerned, the parameters $M_r$ and $B_c$ change less significantly; the most visible effects in this case are slightly steeper fragments of a hysteresis curve associated with magnetic moment flipping.

Figures 9 and 10 present, respectively, how the reduced magnetic remanence $M_r/M_s$ ($M_s$, saturation magnetic moment) and coercive field $B_c$ at the temperature of 2 K depend on concentration for nanoparticles with diameters 3, 6, and 11 nm. It can be seen that s.f. = 2 corresponds to the lowest concentration for which there occur differences

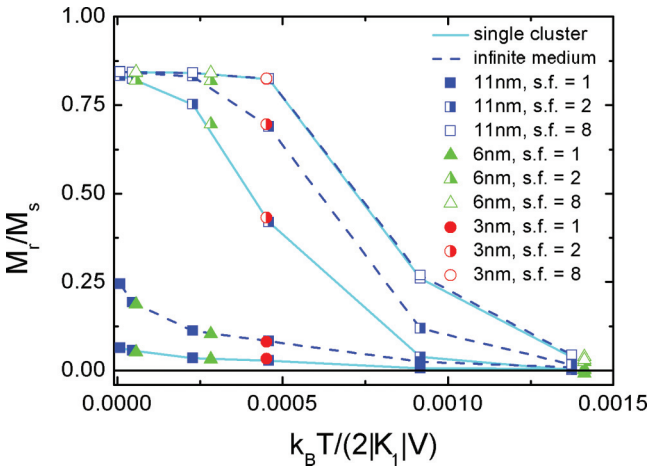


FIG. 11. (Color online) Plot of reduced remanent magnetic moment $M_r/M_s$ versus reduced temperature $k_BT/2|K_1|V$. Sizes of nanoparticles: 3, 6, and 11 nm. S.f. = 1,2,8. Single-cluster calculations are marked with a solid cyan line and periodic system calculations are marked with a dark blue dashed line. For a given diameter, consecutive points are marked for the values of nonreduced temperatures in the sequence 2, 10, 50, 100, 200, and 300 K. 27 nanoparticles, 10 000 MC steps.

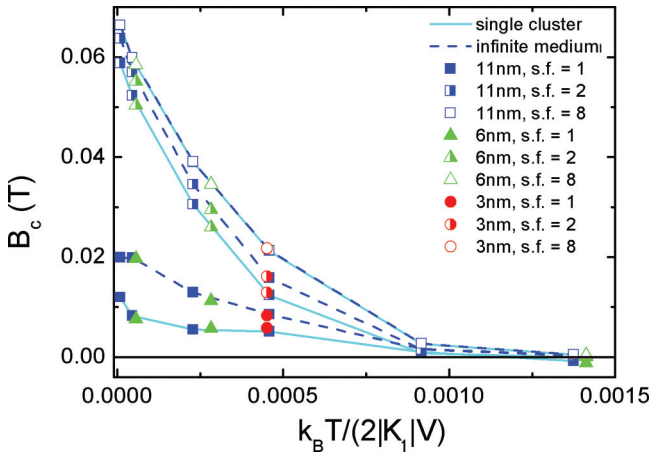


FIG. 12. (Color online) Plot of coercive field ($B_c$) versus reduced temperature $k_BT/2|K_1|V$. Sizes of nanoparticles: 3, 6, and 11 nm. S.f. = 1,2,8. Single-cluster calculations are marked with a solid cyan line and periodic system calculations are marked with a dark blue dashed line. For a given diameter, consecutive points are marked for the values of nonreduced temperatures in the sequence 2, 10, 50, 100, 200, and 300 K. 27 nanoparticles, 10 000 MC steps.

between the results for a single cluster and for an infinite system. These discrepancies, although not very large, are better visible for larger nanoparticles and in the case of higher concentrations, that is, for systems with stronger contribution of the dipole-dipole interactions to the overall energy. For a 3-nm nanoparticle, there is a small difference between the results obtained for an infinite system and for a single cluster. When the diameter increases to 6 or 11 nm, allowing for more long-range dipole-dipole interactions by means of periodic boundary conditions and the Ewald summation procedure causes a slight increase of remanence and coercive field for the cases of s.f. $\leqslant 2$. A similar phenomenon has been observed in calculations for systems of magnetic particles with uniaxial anisotropy.[39,40]

Both $M_r$ and $B_c$ strongly increase with growing s.f. for s.f. $\leqslant 3$ with slightly higher values of $M_r$ and $B_c$ for an infinite system than for a single cluster of nanoparticles, as the consequence of including additional long-range dipolar interactions. For lower concentrations, i.e., for s.f. $\geqslant 3$, no further increase of $M_r$ and $B_c$ with s.f. and no differences between periodic and nonperiodic computations are observed. The dependencies of $M_r$ or $B_c$ versus s.f. are quite similar for large-size nanoparticles, while for the smallest nanoparticles a small minimum appears on the plot of $B_c$ for s.f. = 1.2. Due to the temperature $T = 2$ K chosen for our calculation, we observe size dependence of both $M_r/M_s$ and $B_c$ on particle size. This temperature is close to (but smaller than) $T_b$ for 3-nm particles and much smaller than $T_B$ values for the larger ones.

It was shown[7,21,37] that for an assembly of noninteracting superparamagnetic particles with cubic anisotropy and $K_1 < 0$ in zero temperature $M_r = 0.866$. In the case of s.f. = 8 and $T = 2$ K, variation of $M_r$ for nanoparticles with various sizes becomes very small and magnetic remanence takes values in the range of 0.825–0.844, approaching the specified limit of $M_r = 0.866$. It may also be noticed that remanence decreases with growing concentration. This effect is rather modest if the cases of s.f. = 8 to 2 are compared, but much more pronounced as far as s.f. = 1 is concerned. As it was already stated, this decrease is ascribed to the increasing contribution of the short-range part of dipolar interactions. Similarly, the growth of $M_r$ and $B_c$ for s.f. $\leqslant 2$ after applying periodic boundary conditions can be attributed to the long-range part of the dipole-dipole interactions taken into account by Ewald summation.

### 3. *Universal dependence*

In the graphs presenting reduced $M_r$ and $B_c$ versus $K_BT/2|K_1|V$ (Figs. 11 and 12) reduced temperature is used since in reduced variables curves for various sizes of nanoparticles should overlap. For clarity, all the calculated results are presented only for the 11-nm particles and the values computed for larger reduced $T$ for smaller nanoparticles are not displayed. $M_r$ and $B_c$ were determined for such values of reduced $T$ which correspond in turn to 2, 10, 50, 100, 200, and 300 K. The description of the calculations is made with reference to the values of nonreduced temperature and the points not displayed in the graphs are also considered. In each of the two figures, both periodic (dark blue dashed line) and nonperiodic calculations (cyan solid line) are shown. In fact, in the graphs of reduced $M_r$ and $B_c$ versus reduced $T$, computational points for 3- and 6-nm particles lie on the relevant curves connecting the points obtained for 11-nm particles. Unlike for blocking temperature, in the case of reduced $M_r$, there is a certain increase of values of this quantity after including more dipole-dipole interactions by introducing periodic boundary conditions (Fig. 11). This increase is visible for both s.f. = 2 and for the highest achievable concentration corresponding to s.f. = 1. In the case of s.f. = 8, using periodic boundary conditions and Ewald summation technique has no influence on the values of $M_r$, which is the next proof for the statement that the concentration of nanoparticles is low enough to treat them as a system of noninteracting magnetic dipoles.

The coercive field ($B_c$) shown in Fig. 12 varies as a function of temperature in a similar manner to magnetic remanence. It also grows after adding periodic boundary conditions or increasing interparticle distances. The width of a hysteresis loop diminishes significantly with the increase of temperature. The temperature at which $B_c$ and $M_r$ become close to zero is dependent on the nanoparticles' size determining the blocking temperature at which hysteresis vanishes. In the case of the diameter equal to 3 nm, starting from the temperature of about 10 K, $M_r$ and $B_c$ amount to zero. For a larger diameter of 6 nm, hysteresis is not observed from the temperature of 50 K. In the case of the largest, 11-nm nanoparticles, free rotation of magnetic moments is observed when the temperature reaches 200 or 300 K. The temperature at which $M_r$ and $B_c$ become equal to zero is barely dependent on the scaling factor: only if s.f. = 8 these two quantities fall to zero at slightly higher temperature. It can be concluded that by manipulating the size of nanoparticles or their concentration, one can regulate their hysteresis loop and create a material with adjustable magnetic properties.

## IV. CONCLUSIONS

Monte Carlo simulations of FC/ZFC curves and hysteresis loops were presented for a system of ferromagnetic

nanoparticles. Monodispersed, uniformly magnetized, spherical nanoparticles with cubic anisotropy, randomly distributed and interacting with one another by dipole-dipole interaction, were assumed. Calculations were performed, for example, of fcc-Co nanoparticles. The main goal of the described study is to determine the influence of magnetic dipole-dipole interactions on magnetic properties of the model system at finite temperatures. Calculations were performed for a single cluster of 27 nanoparticles with varying interparticle distances, which allows modification of the strength of magnetic dipolar interactions from corresponding to a densely packed, strongly interacting system up to well-separated noninteracting particles. On the other hand, application of periodic boundary conditions by using Ewald summation allowed us to account for the role of long-range magnetic dipolar interparticle interactions. The magnetic field dependence of blocking temperature and the temperature dependence of magnetic remanence and coercive field, as well as variability of these parameters with changing diameter and concentration of nanoparticles, was also investigated. In order to make a reference to a physical theory, Monte Carlo simulations for a single nanoparticle were supplemented with relevant analytical curves obtained on the basis of Boltzmann distribution. Such calculations performed in the absence of interparticle interactions are also helpful in the description of the remaining contributions to the total energy of a system. The most important observation is the increase of reduced magnetic remanence and coercive field with growing nanoparticle diameter and/or decreasing concentration of nanoparticles. The last feature reflects the importance of dipole-dipole interparticle interaction for dense systems (s.f $< 3$). Consequently, it is predicted that by manipulating the size and/or concentration of nanoparticles, one should be able to obtain nanoparticle systems with tailored properties from hard to soft magnets. Next, the importance of long-range magnetic dipole-dipole interactions is confirmed, as it was observed that applying periodic boundary conditions increases magnetic moment and widens hysteresis loops in the systems with non-negligible interparticle dipole-dipole interactions. On the other hand, increase of short-range dipole-dipole interactions (by making the system more dense and shortening interparticle distances) leads to the opposite effect, i.e., decrease of magnetic moment and coercive field. In the case of concentrations for which magnetic dipolar interactions can be neglected, application of periodic boundary conditions has no effect and reduced magnetic remanence at low temperatures approaches the 0-K limit described in the literature.[37] As far as blocking temperatures are concerned, variation of concentration or application of periodic boundary conditions results in small and irregular changes, while increasing the size of nanoparticles considerably raises $T_b$. It can be thus affirmed that blocking temperature is predominantly influenced by magnetocrystalline anisotropy and hardly affected by interparticle interactions. It is obvious that the presented model, although advantageous as compared to previous ones, is still too simplified to be directly compared to any experimental results. In order to use it for such a purpose, additional effects should be included, i.e., proper distribution of nanoparticle sizes in a sample or decrease of magnetic moment of a nanoparticle due to surface effects. It should be also noted that the investigated system is quite small and the parameters of Monte Carlo simulations are rather suited for the purpose of saving computational time, not for achieving high accuracy of calculations. Considering the discrepancy among values of anisotropy constants for fcc-Co found in the literature, the values used in this work are unlikely to provide a correct fit of computational results to the experimental data for this particular system. However, the presented simulations allow us to predict some general properties of the system without attempting to estimate them quantitatively. For this purpose, the chosen set of parameters seems to be sufficient. In the literature, there are several examples of theoretical investigations of systems of interacting magnetic particles with uniaxial anisotropy.[21,41] However, according to our knowledge, similar computational studies for a system with full cubic anisotropy and interparticle interactions at finite temperature have not been published yet. We believe that the reported results can be of interest from both a theoretical and an experimental point of view and that they can be supportive in the interpretation of magnetic behavior of systems with cubic magnetocrystalline anisotropy. They can be also inspiring in engineering new nanocomposite magnetic materials.

*Corresponding author: jacek.szczytko@fuw.edu.pl

[1]J. Sadowski, E. Janik, E. Lusakowska, J. Z. Domagala, S. Kret, P. Dluzewski, M. Adell, J. Kanski, L. Ilver, R. Brucas, and M. Hanson, Appl. Phys. Lett. **87**, 263114 (2005).

[2]K. Lawniczak-Jablonska, J. Libera, A. Wolska, M. T. Klepka, P. Dluzewski, J. Sadowski, D. Wasik, A. Twardowski, A. Kwiatkowski, and K. Sato, Phys. Status Solidi RRL **5**, 62 (2011).

[3]K. Lawniczak-Jablonska, A. Wolska, M. T. Klepka, S. Kret, J. Gosk, A. Twardowski, D. Wasik, A. Kwiatkowski, B. Kurowska, B. J. Kowalski, and J. Sadowski, J. Appl. Phys. **109**, 074308 (2011).

[4]M. Zajac, J. Gosk, E. Grzanka, M. Kaminska, A. Twardowski, B. Strojek, T. Szyszko, and S. Podsiadlo, J. Appl. Phys. **93**, 4715 (2003).

[5]A. Bonanni, M. Kiecana, C. Simbrunner, T. Li, M. Sawicki, M. Wegscheider, M. Quast, H. Przybylinska, A. Navarro-Quezada, R. Jakiela, A. Wolos, W. Jantsch, and T. Dietl, Phys. Rev. B **75**, 125210 (2007).

[6]A. Bonanni, A. Navarro-Quezada, T. Li, M. Wegscheider, Z. Matej, V. Holy, R. T. Lechner, G. Bauer, M. Rovezzi, F. DAcapito, M. Kiecana, M. Sawicki, and T. Dietl, Phys. Rev. Lett. **101**, 135502 (2008).

[7]L. Tauxe, H. N. Bertram, and C. Seberino, Geochem. Geophys. Geosyst. **3**, 1055 (2002).

[8]W. Gong, H. Li, Z. Zhao, and J. Chen, J. Appl. Phys. **69**, 5119 (1991).

[9]J. P. Chen, C. M. Sorensen, K. J. Klabunde, and G. C. Hadjipanayis, Phys. Rev. B **51**, 11527 (1995).

[10]M. Jamet, W. Wernsdorfer, C. Thirion, D. Mailly, V. Dupuis, P. Melinon, and A. Perez, Phys. Rev. Lett. **86**, 4676 (2001).

[11]C. Thirion, W. Wernsdorfer, M. Jamet, V. Dupuis, P. Melinon, A. Perez, and D. Mailly, J. Appl. Phys. **91**, 7062 (2002).
[12]M. Jamet, W. Wernsdorfer, C. Thirion, V. Dupuis, P. Melinon, A. Perez, and D. Mailly, Phys. Rev. B **69**, 024401 (2004).
[13]A. Aharoni, J. Appl. Phys. **61**, 3302 (1987).
[14]D. A. Garanin and H. Kachkachi, Phys. Rev. Lett. **90**, 065504 (2003).
[15]Y. Labaye, O. Crisan, L. Berger, J. M. Greneche, and J. M. D. Coey, J. Appl. Phys. **91**, 8715 (2002).
[16]G. C. Papaefthymiou, E. Devlin, A. Simopoulos, D. K. Yi, S. N. Riduan, S. S. Lee, and J. Y. Ying, Phys. Rev. B **80**, 024406 (2009).
[17]D. A. Dimitrov and G. M. Wysin, Phys. Rev. B **54**, 9237 (1996).
[18]N. A. Usov and S. E. Peschany, J. Magn. Magn. Mater. **174**, 247 (1997).
[19]J. O. Andersson, C. Djurberg, T. Jonsson, P. Svedlindh, and P. Nordblad, Phys. Rev. B **56**, 13983 (1997).
[20]R. W. Chantrell, N. Walmsley, J. Gore, and M. Maylin, Phys. Rev. B **63**, 024410 (2000).
[21]J. Garcia-Otero, M. Porto, J. Rivas, and A. Bunde, Phys. Rev. Lett. **84**, 167 (2000).
[22]M. El-Hilo, R. W. Chantrell, and K. O'Grady, J. Appl. Phys **84**, 5114 (1998).
[23]C. Verdes, B. Ruiz-Diaz, S. M. Thompson, R. W. Chantrell, and A. Stancu, Phys. Rev. B **65**, 174417 (2002).
[24]O. Chubykalo-Fesenko, K. Guslienko, T. Klemmer, X. W. Wu, R. W. Chantrell, and D. Weller, Phys. B (Amsterdam) **382**, 235 (2006).
[25]S. Russ and A. Bunde, Phys. Rev. B **75**, 174445 (2007).
[26]I. Joffe and R. Heuberger, Philos. Mag. **29**, 1051 (1974).
[27]R. J. Joenk, Phys. Rev. **130**, 932 (1963).
[28]W. A. Sucksmith and J. E. Thompson, Proc. R. Soc. London, Ser. A **225**, 362 (1954).
[29]D. M. Paige, B. Szpunar, and B. K. Tanner, J. Magn. Magn. Mater. **44**, 239 (1984).
[30]P. Ewald, Ann. Phys. (NY) **369**, 253 (1921).
[31]N. Metropolis, A. W. Rosenbluth, A. H. Teller, and E. Teller, J. Chem. Phys. **21**, 1087 (1953).
[32]K. Binder and D. W. Heermann, *Monte Carlo Simulation in Statistical Physics* (Springer, Berlin, 1992).
[33]M. Woińska, A. Majhofer, J. Gosk, and J. Szczytko, Acta Phys. Polon. A **122**, 1019 (2012).
[34]M. P. Allen and D. J. Tildesley, *Computer Simulation of Liquids* (Oxford University Press, New York, 1987).
[35]S. W. D. Leeuw, J. W. Perram, and E. R. Smith, Proc. R. Soc. London, Ser. A **373**, 27 (1980).
[36]Z. Wang and C. Holm, J. Chem. Phys. **115**, 6277 (2001).
[37]R. Gans, Ann. Phys. (NY) **15**, 28 (1932).
[38]S. Bedanta and W. Kleemann, J. Phys. D: Appl. Phys. **42**, 013001 (2009).
[39]D. Kechrakos and K. N. Trohidou, Phys. Rev. B **58**, 12169 (1998).
[40]A. Muxworthy, W. Williams, and D. Virdee, J. Geophys. Res. **108**, 2517 (2003).
[41]M. Porto, J. Appl. Phys. **92**, 6057 (2002).